Hypersonic Aircraft Performance Limitations Arising from Aerodynamic Control Limits

Timothy T. Takahashi[1]
and
Jack A. Griffin[2]

Arizona State University, Tempe, AZ, 85281, US

This paper describes how changes to the aerodynamic configuration of a general-purpose rocket propelled hypersonic aircraft impact its controllability over realistic missions. Aircraft style flight at very high speeds and altitudes requires close attention to: 1) operations at large flight-path angles, 2) high angles of attack to achieve necessary lift under low dynamic pressure conditions and the need for 3) high bank angles to mitigate tendencies for "atmospheric skip." Seemingly stable aircraft may require supplemental reaction-control-jets if its Short-Period and/or Dutch-Roll rigid-body modes fall below fundamental time-domain limits. Other stable aircraft may prove to be uncontrollable using aerodynamic control surfaces alone when the Lateral Control Departure Parameter (*LCDP*) becomes unfavorable. We showcase these issues considering an "astronaut wings" flight flown by the famous North American X-15 rocket plane using both its baseline aerodynamic characteristics as well as variants with differing tail, control and/or wing configurations.

Nomenclature

alt	= altitude, ft
α	= angle-of-attack, deg (°) or radians
b	= span, ft
β	= side-slip-angle, deg (°)
$\bar{c}$	= mean geometric chord, ft
C_L	= coefficient of lift
C_D	= coefficient of drag
$dC_l/dAILERON$	= rolling moment due to aileron defl
$dC_l/d\beta$	= rolling moment due to side slip
$dC_m/d\alpha$	= pitch stability
$dC_n/dAILERON$	= yaw moment due to aileron defl
$dC_n/d\beta$	= yaw moment due to side slip
dELEV	= elevator deflection, deg
Ixx	= rolling moment of inertia, slug-ft^2
Iyy	= pitching moment of inertia, slug-ft^2
Izz	= yawing moment of inertia, slug-ft^2
KEAS	= knots equivalent airspeed
KTAS	= knots true airspeed
M	= Mach number
MTOW	= maximum takeoff weight, lbm
n, nZ	= load factor,-gees
q	= dynamic pressure, lbf/ft^2
S_{ref}	= reference area, ft^2
t	= time, sec
TTD_{sp}	= Short-Period time-to-double, sec
TTD_{dr}	= Dutch-Roll time-to-double, sec
W	= weight, lbm
ω_{sp}	= Short-Period freq, Hz or rad/sec
ω_{dr}	= Dutch-Roll freq, Hz or rad/sec
φ	= bank angle, deg (°)
ρ	= air density, slug/ft^3

[1] Professor of Practice – Aerospace Engineering, School for the Engineering of Matter, Transport and Energy, Arizona State University, Tempe, AZ, 85287. AIAA Associate Fellow.
[2] M.S. Candidate, Aerospace Engineering, Ira A. Fulton Schools of Engineering, Arizona State University, Tempe, AZ, 85287.

©2023 –TT Takahashi & JA Griffin

I. Introduction

HYPERSONIC aircraft imply an ability to cover great ground distances in a brief moment of time. For commercial use, they promise an "Orient Express;" an aircraft that could fly New York to Tokyo in less than two hours. For military use, they promise a nearly invincible weapon; one that could strike a target 500-nM away in less than 10 minutes of flight time. To be truly successful, both military and commercial hypersonic aircraft need to demonstrate positive stability and broad capabilities for controllability across their entire speed envelope.

The North American X-15 rocket plane is an excellent example of a hypersonic winged aircraft, flown by pilots according to aircraft-style flight procedures [1]. In this paper, we use it as a benchmark to extend an aircraft-style time-step integrating mission performance simulation to be able to address the challenges inherent in aero-spaceplane design.

FIGURE 1 – The North American X-15. History's most successful general-purpose powered hypersonic aircraft.

In a previous paper, Griffin & Takahashi [2e] described the enhancements they undertook to a typical point-mass simulation to render it applicable to modelling hypersonic, exo-atmospheric aircraft flight. We implemented the full 1976 standard atmosphere model making the code valid from sea-level to near-space conditions [3]. We incorporated large-angle (rather than small-angle approximate) equations of motion, used the geo-potential gravity model to address flight at very high altitude and also included the centripetal acceleration terms arising from forward flight which oppose gravity. We also implemented an ability to "fly" the aircraft in ballistic and quasi-ballistic flight at atypical load-factors; through "constant α" and "constant CL" flight modes to provide a broader selection of flight styles than that attainable with the typical "level flight" or "climb at constant airspeed" functionality of an airplane style simulation.

While aircraft style point-mass models typically allow flight at $nZ \neq 1$, when extending the simulation we realized that the X-15 flew portions of re-entry at $nZ >> 1$ and at high bank-angles; absent this strategy, the X-15 would "skip" out of the atmosphere during reentry. This strategy requiring high alpha flight at $nZ >>1$ for aerodynamic braking while banking over at a severe angle (φ>45°) enabled the vehicle to decelerate during descent. The fact that the X-15 turns during this maneuver is a byproduct of the need for aerodynamic braking; this is opposite to a typical aircraft – which only inadvertently loses altitude due to a need to change heading.

The X-15 flew at high-speeds both under endo-atmospheric and exo-atmospheric conditions. flights. [4][5][6] Many X-15 trajectories took the aircraft to such altitudes that despite its hypersonic speed, dynamic pressure dropped far below its "1-gee stall speed." "Over-the-top," the X-15 flies a nearly ballistic trajectory that has aerodynamic control diminish to the point of needing reaction control jets for basic attitude, sideslip and roll control. [4] Since the X-15 was intrinsically aerodynamically stable at all speeds and flight attitudes, the need for reaction control jets comes from the time-domain problem. [4] On ascent, as the aircraft progressively flies into a more rarefied atmosphere, the aerodynamically driven rigid-body modes (the Short-Period and Dutch-Roll) diminish to such low frequencies that it becomes impossible to use aerodynamic control with reasonable phase margin to follow the required trajectory. Conversely, on descent, if the aircraft flew in a denser atmosphere at hypersonic speeds, the aerodynamically driven rigid-body modes (the Short-Period and Dutch-Roll) could rise to such a high frequency that they would overlap structural resonances and cause the aircraft to "shake itself to pieces."

In this paper, we will consider the baseline North American X-15 rocket plane configuration, which over its 199 flights proved its fundamental stability. We will also consider the performance of aerodynamic variants with differing tail, control and/or wing configurations. This paper will show how some "aerodynamic improvements" actually lead to a degradation of flying characteristics.

©2023 –TT Takahashi & JA Griffin

II. Populating and Post Processing the Aerodynamic & Mass Properties Database

Flight simulation requires a basic aero data base. The contents of this database consist of functions in terms of the following independent variables. First, there is the weight of the X-15 which varies between its launch weight and its fuel exhausted conditions. Then there is the Mach number which varies from the low subsonic (approach & landing), to the record braking Mach 6+. Last, there is the angle-of-attack which has measures from 0º to 20º; allowing for the high angle-of-attack operations flown during speed bleeding aero-braking maneuvers returning from exo-atmospheric flights. Since the simulation is constantly determining its own conditions, it can perform a trilinear interpolation at flight conditions to extract the desired dependent variables. The dependent variables are trimmed lift coefficient *CL(*M, α), drag coefficient *CD(*M, α), center of gravity location *XCG*(W), moments of inertia *Ixx*(W), *Iyy*(W), *Izz*(W), elevator deflection *dELEV*(M, α), and stability parameters of *dCm/dα*(M,α), *Cnβdynamic*(W,M,α), and *LCDP*(W,M,α).

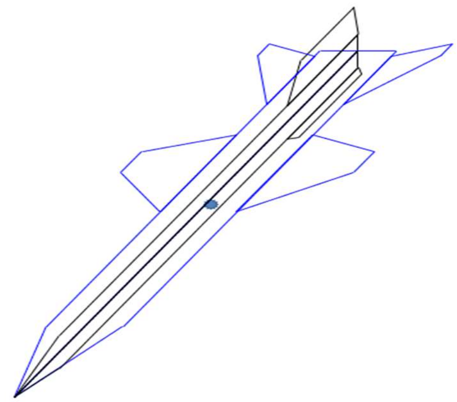

FIGURE 2 – VORLAX model of the Baseline X-15 configuration (small ventral)

A. Calibrating the Basic Model

Our main aerodynamic database derives from a cocktail approach [7] using a Vortex Lattice model [8] of the X-15 (refer to FIGURE 2 for an example), an empirical equivalent flat-plate and form factor zero lift drag estimation [9] and further corrections based on flight test and wind tunnel data.

VORLAX is a vortex lattice potential flow solving CFD code written in FORTRAN and recently received updates that drastically improve performance. [10] VORLAX is especially useful for determining stability derivatives. VORLAX develops influence coefficients for both subsonic and supersonic leading edge flow. We note that its supersonic model only accounts for shock waves developed at the leading and/or trailing edges; as such it is valid for "slender" shapes that do not develop off-body standing shock waves.

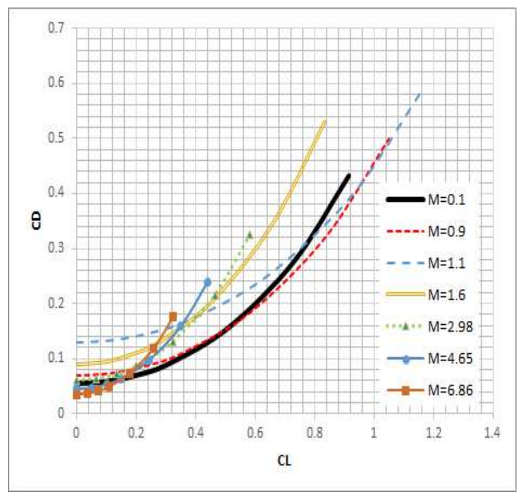

FIGURE 3 – *CD* vs CL from VORLAX "cocktail" aero database (VORLAX with zero-lift-drag offset to match Flight Test data)

While the X-15 was originally conceived to have a symmetrical dorsal and ventral fin, many high-speed X-15 flights were flown with much of the ventral fin removed. The vast majority of wind tunnel data collected represented the initial configuration with the large ventral. [11][12][13] [14][15][16][17][18] Available X-15 wind tunnel data derives from a variety of sources including the NASA/Langley Unitary Plan Wind Tunnel, [14][17] and the NASA/Langley 11-inch hypersonic blowdown tunnel [17][18] among others. Because only a fraction of the total wind tunnel data set modelled the final flight configuration, we began with our Vortex Lattice model of the small ventral flight configuration and "adjusted" the data where necessary (zero-lift drag and wedge-tail-deployed directional stability) to better represent the flight test configuration.

FIGURE 3 plots VORLAX derived estimates of "trimmed" *CD* vs C*L*. We note that there are trust-zone limits *CLmax(*M) for flight at M<1 where *CL* is stall or buffet limited. This is derived from an EDET [26] model of the X-15 and shown in Table 1. For flight at M > 1, the usable aerodynamic database is limited solely by angle-of-attack (0 < α < 20º). In our previous work, [2] we found that the VORLAX model lift-slope closely agreed with Saltzman & Garringer. [19] Since VORLAX is an inviscid code, we adjust its drag estimates with empirical offsets based on the zero-lift-drag established during the X-15's flight test program. [20]

©2023 –TT Takahashi & JA Griffin

B. Longitudinal Stability

As a stable aircraft flies, it will exhibit a natural “bobbing” motion in both a pitching (the “Short-Period”) and in a coupled rolling-and-yawing mode (the “Dutch-Roll”). For an aircraft to be aerodynamically controllable we must have an agreeable short-period frequency. Too fast, and the airplane’s rigid body mode excites structural resonance. Too slow, and the pilot finds the controls to be “mushy” with substantial phase-lag that provokes pilot-induced oscillations.

To estimate the dynamic, rigid-body modes associated with flight, we need to document the pitch responsiveness ($dCL/d\alpha$) and longitudinal stability ($dCm/d\alpha$). In each case, we numerically differentiate data found in our basic aerodynamic database.

To predict the longitudinal “Short-Period” frequency, we use a one-degree-of-freedom dynamic model. The aircraft is represented as a pair of lumped masses (defining the mass-moment-of-inertia) and a torsional spring derived from the aerodynamic stability in pitch, $dCm/d\alpha$; see FIGURE 4. If the system is stable, then there will be some frequency at which it oscillates at, but in the case in which the system is unstable we would like to understand how quickly the system will diverge, a common metric calculated is the time-to-double.

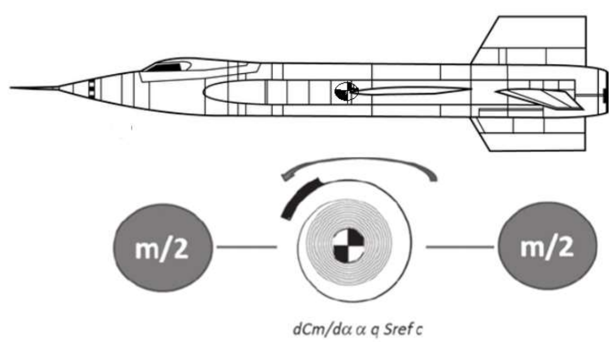

FIGURE 4 – Simplified one-degree of freedom short-period frequency model.

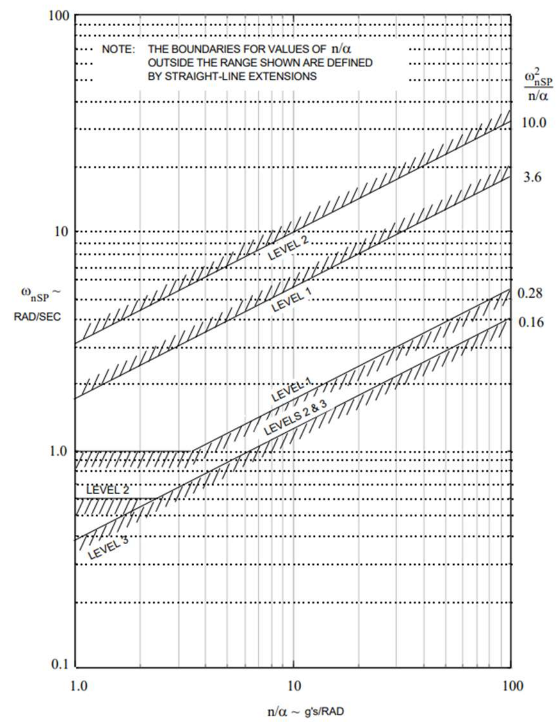

FIGURE 5 - Short Period Frequency Requirements from MIL-8785C

Frequencies for satisfactory flight are outlined in MIL-STD 8785C; see FIGURE 5. [21] The upper bound of the rigid-body “Short-Period” mode is one where the frequency is below that of primary structural resonance; typically, this will be a single digit frequency in Hz (i.e. 3-Hz) as predicted by structural finite-element-analysis. It is possible for this condition to develop when a very stable aircraft flies at extremely high dynamic pressure (*KEAS* >> 1000).

MIL-STD 8785C defines aircraft into several classes based on their size and intended purposes: there are three categories of nonterminal flight of which we focus primarily on Category A. Category A flight implies active maneuvering whereas Category B is defined as “Climb” “Cruise” and “Loiter” (less demanding piloting conditions) or Category C which is defined for takeoff & landing (and is even more demanding to pilot). The primary X-15 flight falls under the Category A condition; refer back FIGURE 5.

©2023 –TT Takahashi & JA Griffin

MIL-STD 8785C defines three levels of "handling qualities" representing pilot workload as defined by the Short-Period frequency and pitch responsiveness of the airframe: *LEVEL 1* where the qualities are clearly adequate, *LEVEL 2* where flying qualities are adequate but requires a higher workload, and *LEVEL 3* where the aircraft is still safe but requires excessive workload.

From these specifications we will be able to analyze the characteristics of a high-speed aircraft, like the X-15 as it flies its mission.

MIL-STD 8785C (refer once again to FIGURE 5) stipulates *LEVEL 1* qualities if the longitudinal parameter $\omega^2_{sp}/(n/\alpha)$ falls in the range $0.28 < \omega^2_{sp}/(n/\alpha) < 3.6$; with a floor of $\omega_{sp} = 1$ radian/sec (0.16 Hz or a 6.28 second Short-Period mode). *LEVEL 2* qualities if $0.16 < \omega^2_{sp}/(n/\alpha) < 3.6$; with a floor of $\omega_{sp} = 0.6$ radian/sec (0.095 Hz or a 10.5 second Short-Period mode). *LEVEL 3* qualities exist so long as $\omega^2_{sp}/(n/\alpha) > 0.16$. If $\omega^2_{sp}/(n/\alpha) < 0.16$ the standard deems the aircraft unacceptably unresponsive.

Because the previously stated stability parameters depend on flight conditions, weight and moments of inertia, we must calculate them in the context of a proposed flight trajectory. Since flight conditions are continuously tracked by the point-mass kinematics of the mission code, we know the Mach #, angle-of-attack (α), dynamic pressure and flight weight at each time step. From there, we can estimate pitch responsiveness at each time step along the trajectory as:

$$\frac{n}{\alpha} \approx \frac{57.4\frac{dCL}{d\alpha} q\, Sref}{W} \tag{2}$$

In order to estimate the Short-Period frequency at each time step along the trajectory, we will need to estimate the mass-moment-of-inertia in pitch (*Iyy*) as a function of flight weight; we currently use simple linear interpolation. From there, we can estimate the Short-Period Frequency in Hz as: [22]

$$\omega_{sp} \approx \left(\frac{1}{2\pi}\right)\sqrt{\frac{-57.3 \cdot dC_m/d\alpha \cdot q \cdot S_{ref} \cdot \bar{c}}{I_{yy}}} \tag{3}$$

The X-15, along with many Hypersonic Boost-Glide concepts, flew at extremely high altitudes. Despite the high Mach number, the vehicle may actually fly a substantial portion of its mission at low dynamic pressure. Thus, we must consider the lower bounds of longitudinal responsiveness. To do so, refer one last time to the MIL 8785C chart (FIGURE 5). As the aircraft leaves the atmosphere and q heads towards zero, n/α also heads towards zero. Note that if $n/\alpha \sim 1.0$-gee/radian (the lower bound of the chart) this metric implies trimmed flight at 1-gee (i.e. $nZ = 1$) to require 57.4 º angle-of-attack. So, the practical limit to trimmed (rather than quasi-ballistic flight) exists so long as $n/\alpha > 3$ (i.e. when 1-gee trimmed flight can exist at less than ~20º angle-of-attack).

For quasi-ballistic flight, where the aircraft may operate at or below $n/\alpha \sim 3$, we see that the minimum permissible *LEVEL 3* Short-Period frequency is ~0.4 radian/sec (0.06-Hz or a 15-second period). When the rigid body frequencies drop below that, the aircraft becomes hopelessly unresponsive to pilot using a conventional control strategy. If our mission code indicates such slow rigid body modes as the aircraft leaves the atmosphere, the GNC system will need to abandon an aerodynamic control approach and revert to reaction-control jets.

C. Assessing the Lateral-Directional Stability & Controllability

We next turn to the lateral-directional stability and controllability of the airframe. First, we will assess the stick-fixed lateral-directional stability as it pertains to the Dutch-Roll rigid body mode. Secondly, we will assess if the aerodynamic roll-control strategy implied by the control surface disposition unintentionally makes the aircraft prone to spin.

The basic stick-fixed lateral-directional stability as predicted by VORLAX may be seen in FIGUREs 6 and 7, overleaf. The "lower-rudder-off" configuration has weakly positive directional stability ($dCn/d\beta > 0$) with rising stability up to Mach 1.6. Above this speed, the X-15 deploys its wedge "speed brake" to enhance directional stability to a level of $dCn/d\beta \sim +0.008$. Under all positive attitudes, the X-15 displays stabilizing effective dihedral ($dCl/d\beta < 0$).

©2023 –TT Takahashi & JA Griffin

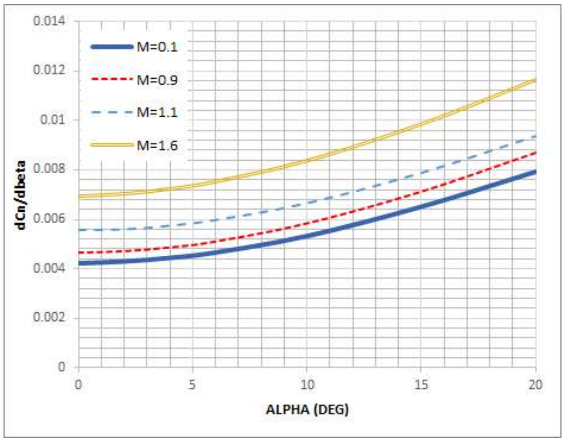

FIGURE 6 – dCn/dβ vs alpha from VORLAX

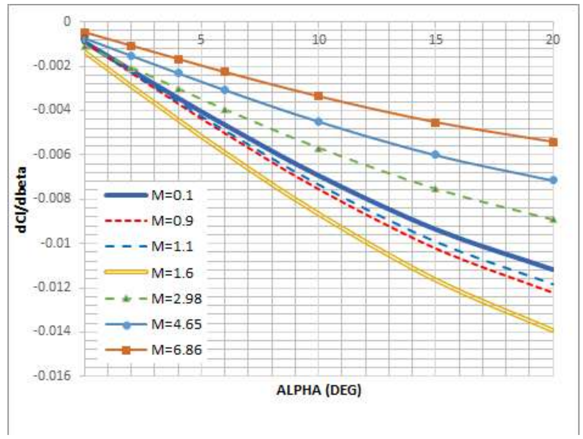

FIGURE 7 – dCl/dβ vs alpha from VORLAX

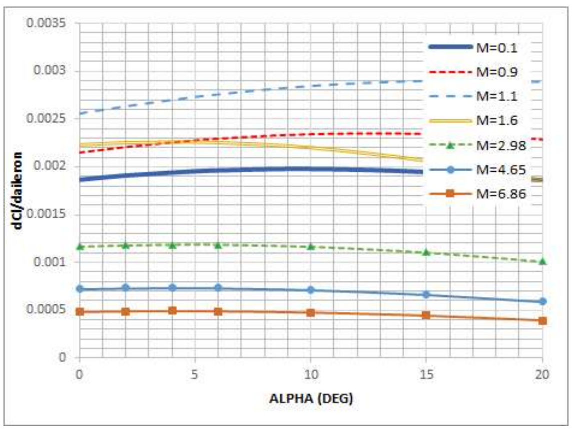

FIGURE 8 – dCl/dAILERON for differential elevator deflections from VORLAX

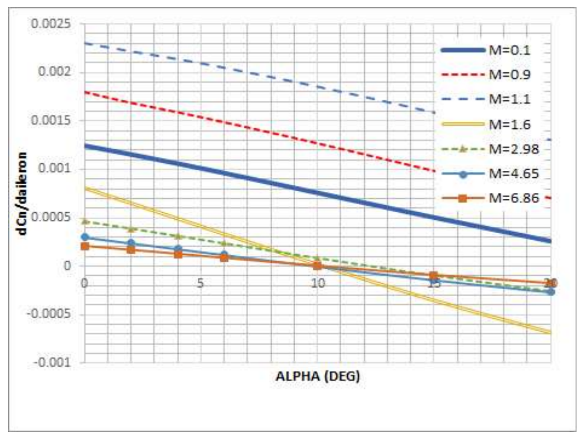

FIGURE 9 – dCn/dAILERON for differential elevator deflections from VORLAX

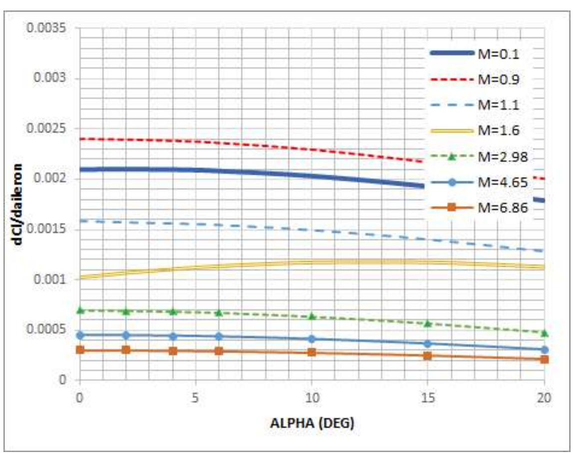

FIGURE 10 – dCl/dAILERON from a wing mounted aileron

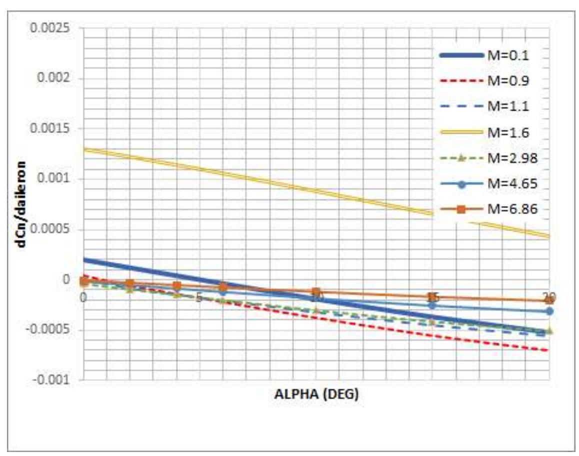

FIGURE 11 – dCn/dAILERON from a wing mounted aileron

FIGUREs 8 through 11 show the "aileron" effect to command aircraft roll accomplished through two difference design strategies. FIGUREs 8 and 9 roll the airframe through differential deflection of the X-15's horizontal tail "elevon" surfaces. FIGUREs 10 and 11 roll the airframe through differential deflection of hypothetical wing mounted ailerons. In all cases, the plots show the change in roll and yaw coefficients as a result of a +/- 1° anti-symmetric deflection of

©2023 –TT Takahashi & JA Griffin

the control surfaces. The choice of control surfaces produces roughly equivalent roll control power, but the wing mounted ailerons produce substantially more adverse yaw (when *dCn/dAILERON* has an opposite sign to *dCl/dAILERON*) than the differential elevator. This distinction will prove an important reason why the production X-15 did not employ wing mounted ailerons.

In order to estimate Dutch-Roll lateral directional stability and spin resistance, we need to compute $C_n\beta$ *dynamic* and the lateral-control-departure-parameter, *LCDP*.

To compute $C_n\beta dynamic$ was must first transform all of the lateral-directional moments into wind axis and then scale $dCl/d\beta$ by the ratio of rolling moment of inertia to yawing moment of inertia:

$$C_n\beta dynamic = \frac{dC_n}{d\beta}\cdot\cos(\alpha) - \frac{dC_l}{d\beta}\cdot\left(\frac{I_{zz}}{I_{xx}}\right)\cdot\sin(\alpha) \quad (5)$$

For an aircraft to be aerodynamically controllable, it must also have an agreeable Dutch-Roll frequency. Too fast, and the airplane's rigid body mode excites structural resonance. Too slow, and the pilot finds the roll response to be "mushy" with substantial phase-lag that provokes pilot-induced oscillations. MIL STD 8785C [21] supplies a floor of ~0.4 radians/sec for the lateral-directional Dutch-Roll frequency (that is 0.064 Hz or a 15 second period). When the rigid body frequencies drop below that, the aircraft becomes too unresponsive to pilot with a conventional control strategy. For an exo-atmospheric aircraft like X-15, as the frequencies drop too low the aircraft needs to transition to a reaction control system (RCS) to maintain attitude control. [24]

In order to approximate the Dutch-Roll frequency, we may use a 1-degree-of-freedom simplification where we consider the rigid body aircraft as a pair of lumped masses (defining the mass-moment-of-inertia) and a torsional spring (driven by $Cn\beta dynamic$). This leads to the simplified Dutch-Roll equation [22][23] for an inherently stable system:

$$\omega_{dr} \approx \left(\frac{1}{2\pi}\right)\sqrt{\frac{57.4\cdot C_n\beta\ dynamic\cdot q\cdot S_{ref}\cdot b}{I_{zz}}} \quad (6)$$

In the Dutch-Roll is unstable, we will then use the following equation to estimate the unstable "time-to-double" response:

$$TTD_{dr} \approx \sqrt{\frac{I_{zz}}{-57.4\cdot C_n\beta\ dynamic\cdot q\cdot S_{ref}\cdot b}} \quad (7)$$

Lastly there is the Lateral Control Departure Parameter – the lateral control departure parameter – if *LCDP* < 0, the adverse yaw from the roll control surfaces overwhelms the static lateral-directional stability of the aircraft precipitating a spin and loss of control. [23] *LCDP* is found using the following equation:

$$LCDP\ = \frac{dC_n}{d\beta} - \frac{dC_l}{d\beta}\cdot\frac{\left(\frac{dC_n}{d\ aileron}\right)}{\left(\frac{dC_l}{d\ aileron}\right)} \quad (8)$$

The reader should understand that if either the rigid body frequencies **or** *LCDP* falls below minimums, we must either avoid the flight regime or transition to a reaction control jet system to prevent a loss of control. [23][24]

As with longitudinal stability, low frequency conditions will be found "over-the-top" during exo-atmospheric flight where $q \rightarrow 0$ while rigid body modes likely to provoke structural resonance will be found during high-speed low-altitude flight where *KEAS*>>1000.

©2023 –TT Takahashi & JA Griffin

III.Trade Study Aerodynamic Data

This paper examines the impacts of configuration aerodynamic decisions made during the X-15 program.

The baseline flight test (see FIGURE 12a) X-15 features a *Sref* ~ 200-ft^2 thin wing lacking any control surfaces, pitch and roll control from a thin all moving horizontal tail and directional stability and control implemented through a large dorsal and small ventral wedge shaped vertical tail. The upper portion of the dorsal can swivel to act as a rudder. The lower portion of the dorsal and the ventral were fitting with deployable “speed brakes” that significantly increased the static directional stability of the airframe at only a modest impact to zero-lift-drag at high supersonic speeds.

The proposed X-15-3 (see FIGURE 12b) X-15 features a stretched fuselage and slender delta wing with aft mounted elevons for both pitch and roll control. Directional stability and control implemented through a large dorsal, small ventral and a pair of wingtip mounted supplemental wedge shaped vertical fins. The upper portion of the dorsal can swivel to act as a rudder. The lower portion of the dorsal and the ventral were fitting with deployable “speed brakes” that further increased the static directional stability of the airframe at only a modest impact to zero-lift-drag at high supersonic speeds. Our estimates predict that the X-15-3 is roughly twice as directionally stable as the baseline X-15 at high supersonic speeds.

We will consider four configurations including the production X-15 airframe; FIGURE 13 depicts the gamut of aerodynamic models examined in this paper. We may consider the performance of the baseline configuration, flown on a hypersonic “astronaut’s wings” mission; see FIGURE 13a. We also can consider a slight variation on this configuration: if the designer was to omit the deployable “speed brakes” and use a more conventional airfoil section for the vertical and revert to classic wing mounted ailerons, would this improve or detract from high speed controllability? (it would surely reduce airframe and controls complexity) FIGURE 13b shows a simplified version of the proposed X-15-3 configuration, with the large delta wing and a simple vertical, but omitting the supplemental wingtip fins. Finally, FIGURE 13c sketches the final proposed X-15-3 configuration with large supplemental wingtip fins as well as the central dorsal and ventral wedge fins with deployable speed brakes.

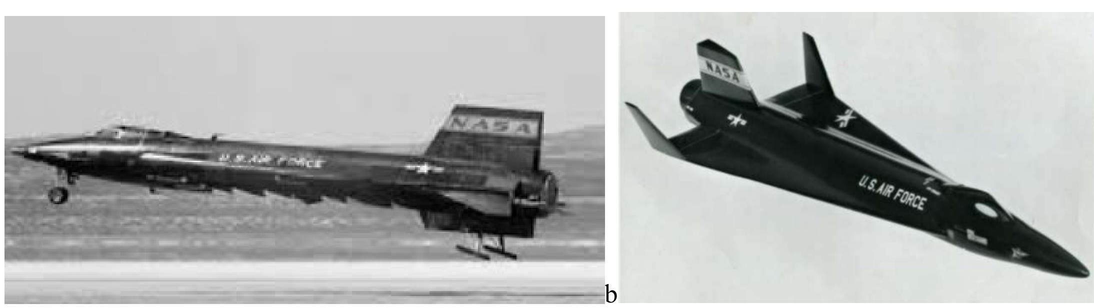

FIGURE 12 - X-15 Aerodynamic Configuration - a) baseline w/ small ventral, b) large delta wing w/ triple verticals

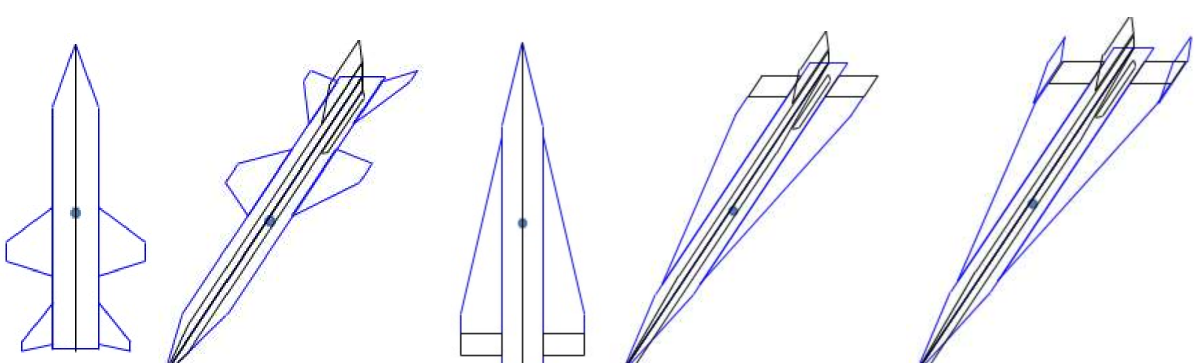

a b c

FIGURE 13 - X-15 VORLAX Models - a) baseline, b) large delta wing w/o supplemental verticals, c) large delta wing w/ triple verticals

©2023 –TT Takahashi & JA Griffin

FIGURE 14 is a plot of the basic longitudinal aerodynamic data for the two basic configurations. For simplicity in drag calibration, we hold Sref constant between all databases despite the large change in wing area. In FIGURE 14a, we see CL vs α for the basic X-15 configuration. These VORLAX predictions, as noted above, closely matched wind tunnel and flight data from actual X-15 missions. As the Mach number increases, the slope of CL vs α first increases (following the Prandtl-Glauert rule) than decreases (following the Ackeret rule). FIGURE 14b, with the larger physical delta wing employing much greater sweep but unchanged reference area shows a much steeper slope at all speeds. Thus, the "big-wing" on the X-15-3 could sustain higher flight weights at equivalent dynamic pressure conditions.

FIGURE 15 shows the drag-due-to-lift and zero-lift-drag trends for the two basic configurations. The large, delta wing generates much more lift without a substantial increase in zero-lift-drag. Thus, the large wing configurations imply a vehicle with an improved hypersonic lift-to-drag ratio that may improve its kinematic mission performance.

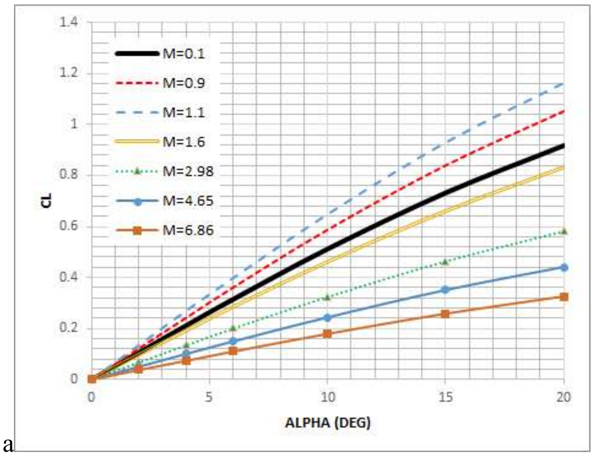

a

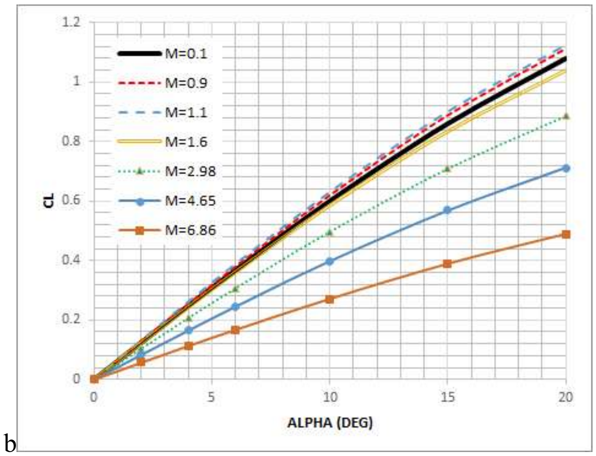

b

FIGURE 14 - X-15 & Derivatives Aerodynamic Data – CL vs alpha – a) baseline wing, b) large delta wing

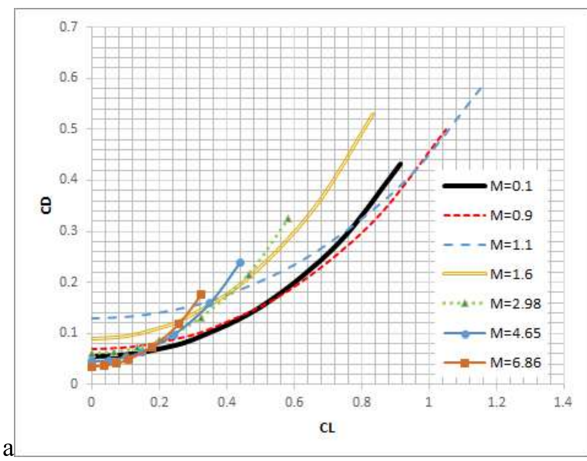

a

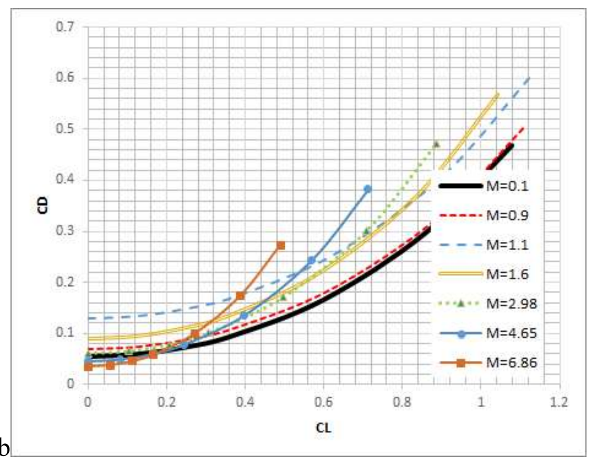

b

FIGURE 15 - X-15 & Derivatives Aerodynamic Data – CL vs CD – a) baseline wing, b) large delta wing

©2023 –TT Takahashi & JA Griffin

Turning next to FIGURE 16 we can examine the static lateral-directional stability of the four proposed configurations. All figures demonstrate a vehicle with strong positive lateral-directional stability which only increases with angle-of-attack; this implies a stable Dutch Roll mode under all flight conditions. Comparing the small wing (FIGURE 16a and 16b) to the large delta wing (FIGUREs 16c and 16d) configurations, we see that the large delta wing increases *Cnβdynamic* substantially. Comparing the thin-vertical (FIGURES 16b and 16c) to the wedge vertical (FIGURES 16a and 16d) cases, we see that the strong increase in hypersonic static directional stability makes only a small difference in the magnitude of *Cnβdynamic*. For these shapes the majority of the Dutch Roll stability comes from its effective dihedral ($dCl/d\beta<0$) not from its static directional stability ($dCn/d\beta>0$), We may then ask what was all of the fuss about with the wedge tails for the flight test X-15 (configuration a) or the proposed X-15-3 (configuration d). Did the designers like complexity or have a stylistic fascination with wedge shaped airfoils?

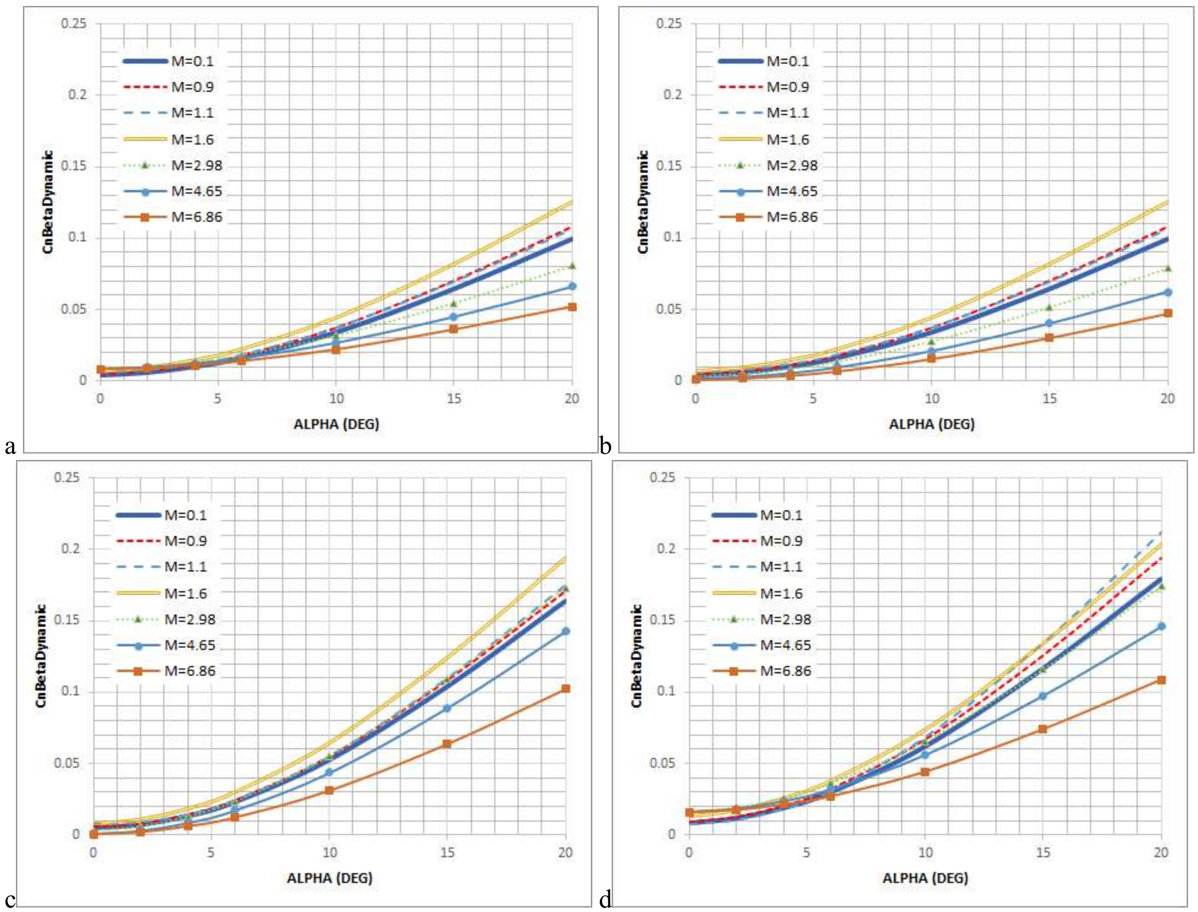

FIGURE 16 - X-15 & Derivatives Aerodynamic Data – CnβDynamic– a) baseline wing w/ wedge tail and differential elevon for roll, b) baseline wing w/ thin vertical, c) large delta wing w/ thin vertical, d) large delta wing w/ triple wedge verticals

©2023 –TT Takahashi & JA Griffin

In retrospect, the enhanced static directional stability of the proposed and produced airframes was needed to prevent an "aileron" induced loss of control. If we turn next to FIGURE 17, we can examine the *LCDP* stability of the four proposed configurations. Here the configurations differ widely from one another. The "as-flown" X-15 baseline configuration with the small ventral fin shows positive *LCDP* across all speeds and angles-of-attack; see FIGURE 17a. If we were to weaken the static directional stability at high speeds by eliminating the wedge vertical and "speed brakes" and to change the adverse-yaw properties of the roll control devices by implementing wing mounted ailerons in lieu of differential aft elevator, we see generally promising *LCDP* at M<1.6 but declining characteristics ($LCDP$ < 0) as we attempt hypersonic flight (M>4) at the high angles of attack (α>10-deg) needed to fly atmospheric re-entry; see FIGURE 17b. Similarly, unfavorable *LCDP* is obvious with the large delta wing at high speeds (see FIGURE 17c); thus the need to festoon the rear of the X-15 with dorsal wedge fins and speed brakes becomes obvious. Even with substantially larger vertical fins, *LCDP* is favorable on the proposed X-15-3 configuration at hypersonic speeds if we limit α<~18-deg; see FIGURE 17d. It seems like a hypersonic maneuvering vehicle can't have enough static directional stability at high speeds and angles of attack.

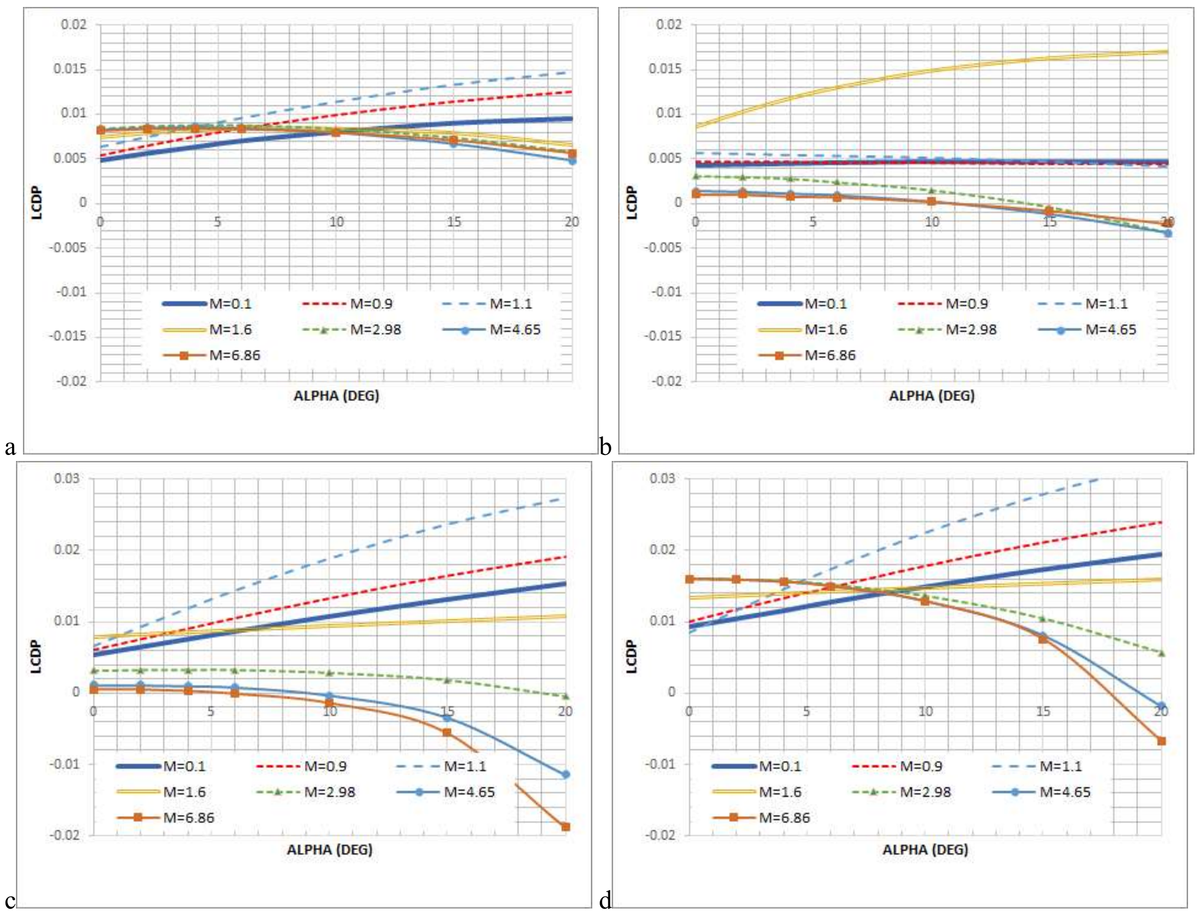

FIGURE 17 - X-15 & Derivatives Aerodynamic Data – *LCDP*– a) baseline wing w/ wedge tail and differential elevon for roll, b) baseline wing w/ thin vertical and wing mounted ailerons for roll, c) large delta wing w/ thin vertical, d) large delta wing w/ triple wedge verticals

©2023 –TT Takahashi & JA Griffin

IV. Comparison over a Reference Mission

To see how the stability changes with alternative designs impacts the operational utility of the X-15, we will "fly" a demanding exo-atmospheric mission using our mission simulation code. In each case, the basic mission profile and the five-column propulsion data are left untouched. The baseline performance aerodynamics database is compared to the large delta wing with thin vertical, large delta wing with triple verticals, and thin vertical and wing mounted ailerons for roll (Trade 3); refer back to FIGURE 13 to compare these configurations.

Our reference mission broadly follows the 'HIGH ALTITUDE' case found in NASA TM X-638 [25]; see FIGURE 19. This case was chosen for its exo-atmospheric flight and hypersonic flight. It begins with an air-drop launch around ALT=45,000-ft / M=0.8 followed by a near ballistic climb up out of the atmosphere. For most of the flight, the angle-of-attack is the controlled variable.

Flight "over the top" will be at a negligible dynamic pressure.

Re-entry will involve a significant nose-up attitude as well as bank angle in order to avoid an atmospheric skip. This maneuver means that an actual X-15 trajectory will differ from that in the conops sketch; the re-entry will not be flown in a straight line down range but will incorporate a distinct turn. It is clear to us from a review of X-15 flight test data that this was a necessary part of real flights. [11][25][26]

The result of this profile can be seen plotted on top of the actual data in FIGURE 20, overleaf. For the baseline vehicle, we can see that there is very good agreement between the simulated and actual flown trajectory. For the X-15-3, the larger wing leads to higher peak altitudes and lower peak speeds both on ascent and during re-entry.

While the X-15-3 can certainly be flown in a manner that would increase its top speed, we consider this reference trajectory still useful to assess stability and control concerns.

Minor changes in vertical tail configuration and control surface disposition do not materially impact the trajectory. If we compare FIGURE 20a vs 20b, we see negligible differences whether the vertical tail is a wedge or not and whether roll control is implemented with differential elevon or with discrete ailerons. We do consider that the drag increment of the speed brakes (the variable wedge angle vertical tail on the actual X-15) remains unchanged between the two candidate configurations. If we compare FIGURE 20c vs 20d, we see negligible differences arising from the increased directional stabilizing area on the triple wedge vertical variant.

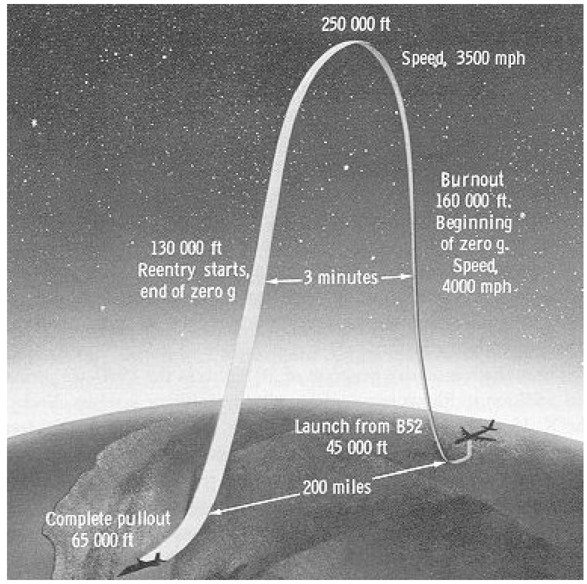

FIGURE 18 – X-15 ConOps

Segment	Condition
0→1	Air Drop at Mach ~ 0.8, ALT~45,000-ft; ignite motor and pitch up at constant α = 6°, Until > 125,000-ft, then cutoff motor
1→2	*PLA* = 0, Constant α = 6°, Until *ALT* > 200,000-ft
2→3	*PLA* = 0, Constant α = 5°, Deploy Brakes, Until < 160,000-ft
3→4	*PLA* = 0, Constant α = 16°, Until Mach < 4.5
4→5	*PLA* = 0, Constant α = 16°, Bank 45°, Until Mach < 4
5→6	*PLA* = 0, Constant α = 14°, Bank 70°, Until Mach < 3.5
6→7	*PLA* = 0, Constant α = 12°, Bank 70°, Until Mach < 3
7→8	*PLA* = 0, Constant α = 10°, Bank 60°, Stow Brakes, Until Mach < 2
8→9	*PLA* = 0, Wing Level Decelerate, Until *KIAS* < 225-knots
9→	*PLA* = 0, Descend at Constant *KIAS*

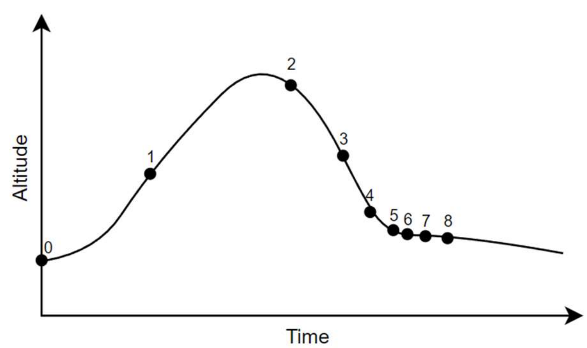

FIGURE 19 – NASA TM X-638 Trajectory [26]

©2023 –TT Takahashi & JA Griffin

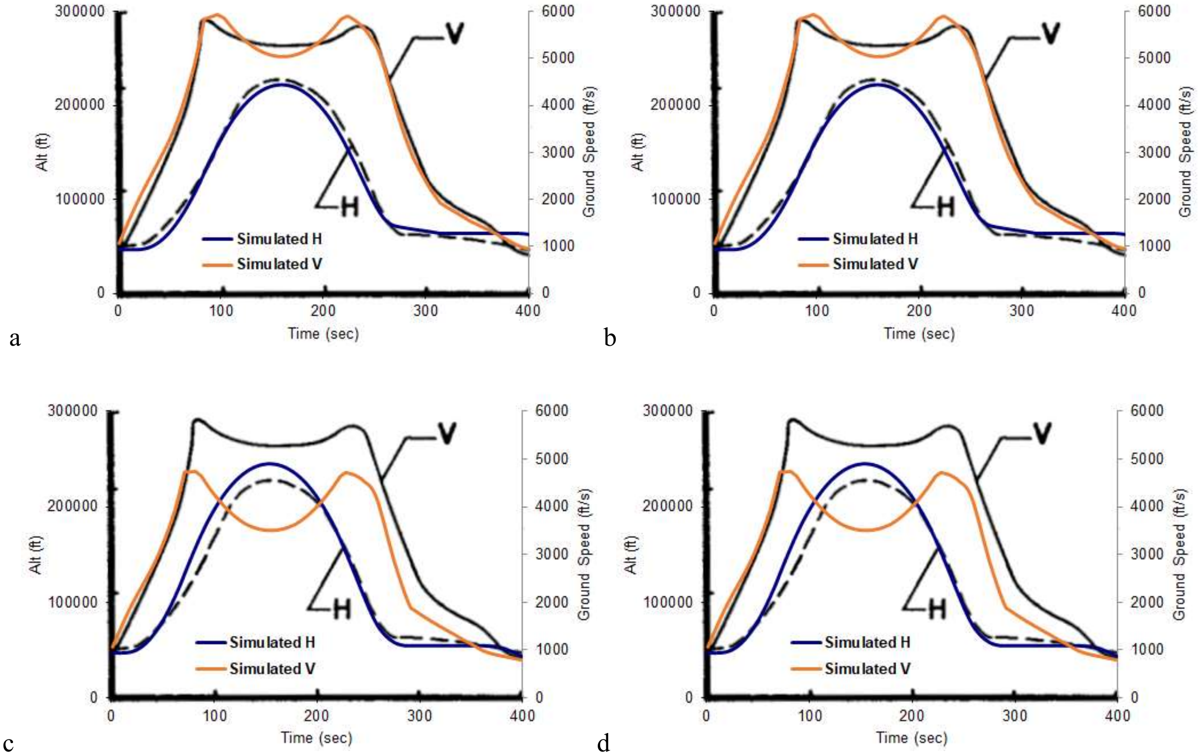

FIGURE 20 – X-15 & Derivatives Performance Baseline – Altitude and Speed vs Time - a) calibrated X-15 baseline wing w/ wedge tail and differential elevon for roll, b) baseline wing w/ thin vertical and wing mounted ailerons for roll, c) large delta wing w/ thin vertical, d) large delta wing w/ triple wedge verticals

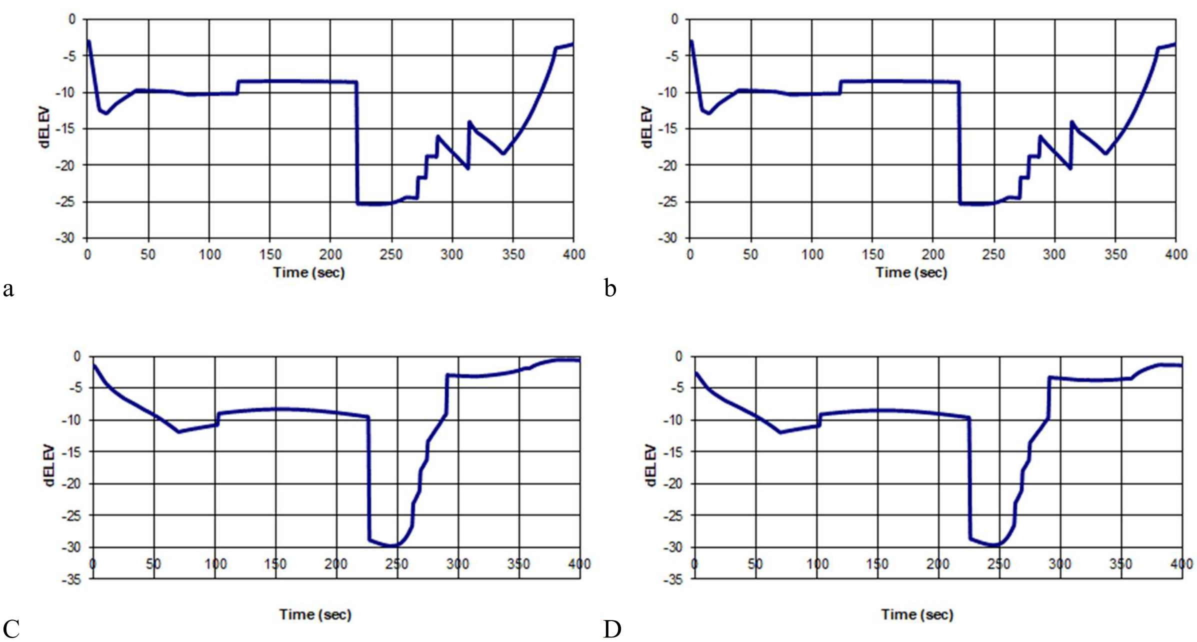

FIGURE 21 – X-15 & Derivatives Performance Baseline – Elevator to Trim vs Time - a) calibrated X-15 baseline wing w/ wedge tail and differential elevon for roll, b) baseline wing w/ thin vertical and wing mounted ailerons for roll, c) large delta wing w/ thin vertical, d) large delta wing w/ triple wedge verticals

©2023 –TT Takahashi & JA Griffin

Turning next to FIGURE 21 (prior page), we can see that that changes in vertical (compare 21a with 21b and 21c with 21d) tail surface area and roll control effector geometry do not impact the ability for the X-15 to trim in pitch. FIGURE 21 shows that the major changes to planform i.e. the delta wing do make a significant difference. At the analyzed CG position, the X-15-3 requires more control surface deflection to trim during re-entry (~30º) than does the baseline (~25º). Given that the X-15-3 does not include a discrete roll effector, and thus differential elevon will be needed to aerodynamically command roll during re-entry, this configuration is likely to lead to control surface saturation problems. With only an approximate CG position known for this proposed configuration, we speculate that an "as-built" X-15-3 would have flown with a CG somewhat aft of our analysis point. A slight rearward shift in CG would reduce the static longitudinal stability and thus would reduce the longitudinal control power required at the expense of slowing the stick-fixed rigid body longitudinal mode.

Moving on to FIGURE 22, we can see that the differences between the proposed configurations in terms of the 8785C longitudinal frequency / pitch responsiveness charts is not large. So long as the dynamic pressure is high enough to permit reasonable pitch responsiveness, all proposed configurations lie within the LEVEL 1 handling quality region. All configurations share the same issue; that "going over the top" will require a propulsive reaction control system as both the pitch responsiveness and the longitudinal rigid-body modes drop to nothing as the X-15 leaves the atmosphere.

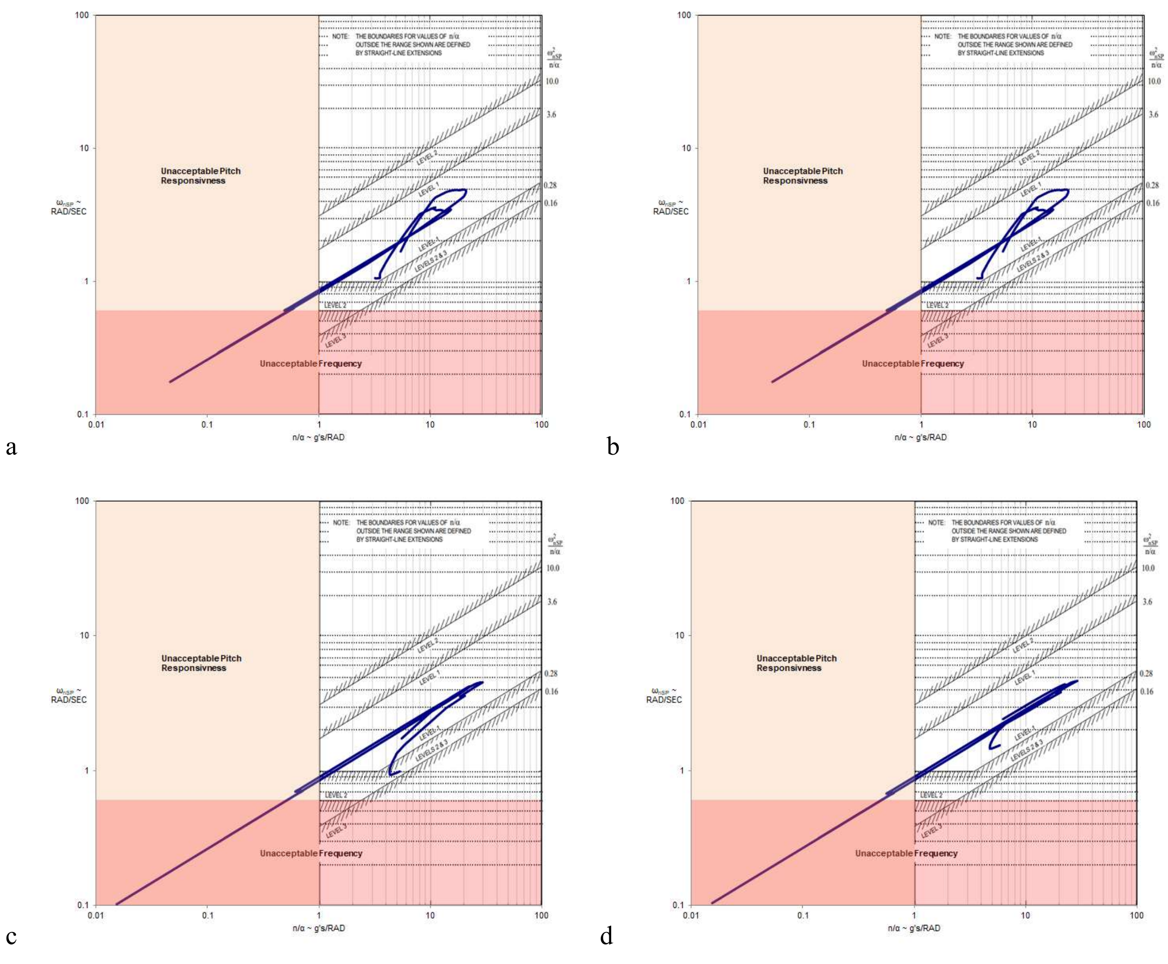

FIGURE 22 – X-15 & Derivatives Performance Baseline – 8785C ωsp vs n/α - a) calibrated X-15 baseline wing w/ wedge tail and differential elevon for roll, b) baseline wing w/ thin vertical and wing mounted ailerons for roll, c) large delta wing w/ thin vertical, d) large delta wing w/ triple wedge verticals

©2023 –TT Takahashi & JA Griffin

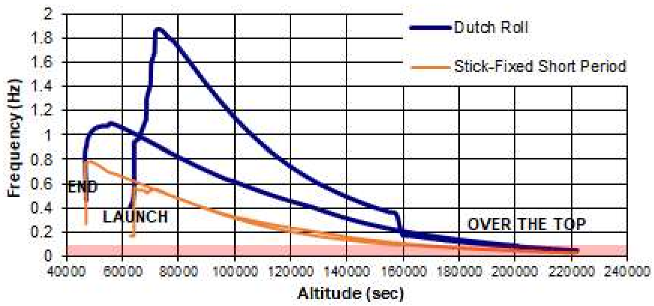

a

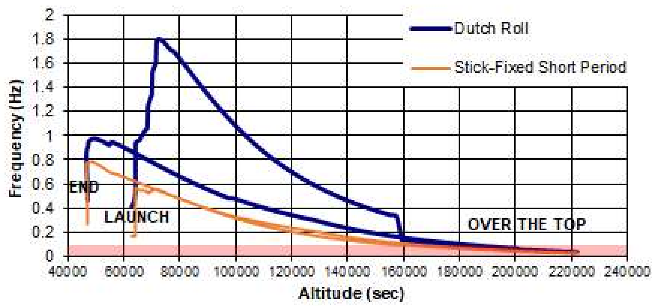

b

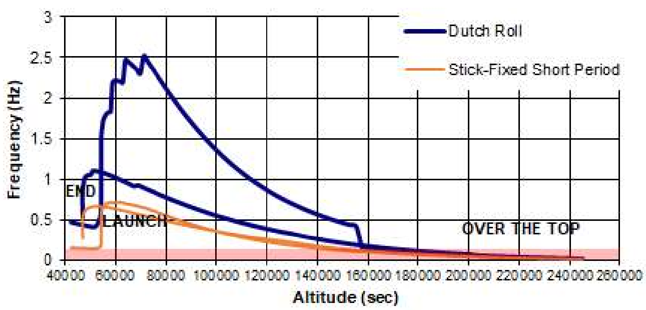

c

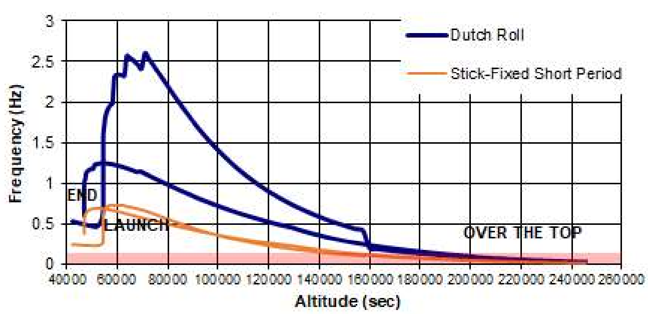

d

FIGURE 24 – X-15 & Derivatives Performance Baseline – Short Period & Dutch Roll Freq. vs Alt - a) calibrated X-15 baseline wing w/ wedge tail and differential elevon for roll, b) baseline wing w/ thin vertical and wing mounted ailerons for roll, c) large delta wing w/ thin vertical, d) large delta wing w/ triple wedge verticals

Consider the Dutch Roll modes with FIGURE 24. It shows how the aerodynamic configuration, straight wing or delta, drives the Dutch Roll frequencies. The delta wing, see FIGURE 24c and 24d, has more effective aerodynamic dihedral, and hence a faster Dutch Roll mode than the baseline. Thus, the structural design teams needs to be aware that delta configurations can express Dutch Roll frequencies > 2-Hz; this may be high enough to excite structural resonance. We see the Short Period and Dutch Roll modes "crossing" one another (a region where aerodynamic "inertia coupling" would develop) briefly at the start and end of endo-atmospheric flight. As we go "over the top," both Dutch Roll and Short Period frequencies drop to near zero – thus while "inertial coupling" may theoretically develop there, it is during a phase of flight where the aircraft will already be needing RCS for stabilization and control.

Finally, we must consider control coupling; turn to FIGURE 25, overleaf. If *LCDP* goes negative, any aerodynamic attempt to command a roll develops sufficient adverse yaw to overpower static directional stability and provoke a spin. We can see over the analyzed trajectory the "as-flown" X-15 baseline and the proposed X-15-3 with three verticals express *LCDP*>0.; the X-15-3 with triple verticals is better than the baseline. So long as the dynamic pressure is high enough not to need RCS, both of these configurations appear to be safe and controllable entirely through aerodynamic control.

For the discarded alternative configurations, neither the basic X-15 with a conventional vertical tail and wing mounted ailerons nor the X-15-3 delta wing lacking the triple tails appears safe through aerodynamics control alone. Returning to FIGURE 25, note that for both configurations *LCDP* is nearly zero from 6< t < 200-sec; the whole ascent as well as "over the top." These configurations also express control induced spin tendencies with negative *LCDP* 240<t<270-sec during re-entry, precisely when the aileron control is need to hold a severe bank angle to prevent an atmospheric skip. In order to avoid a spin, these vehicles would need to employ RCS to counteract the adverse yaw of the ailerons during endo-atmospheric flight at high dynamic pressure.

©2023 –TT Takahashi & JA Griffin

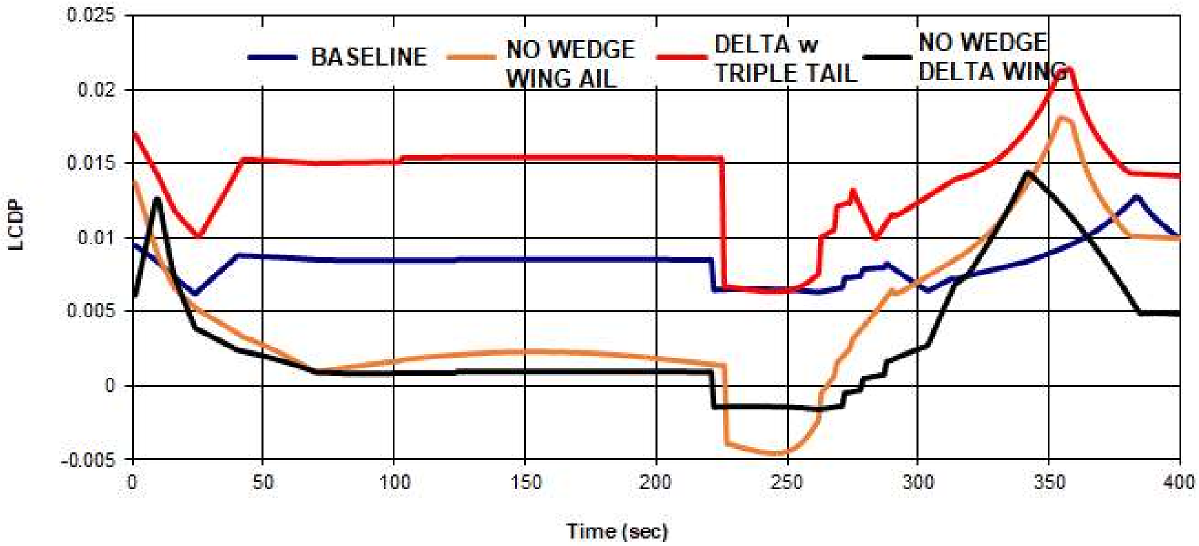

FIGURE 25 – X-15 & Derivatives Performance Baseline – *LCDP*. vs time - a) calibrated X-15 baseline wing w/ wedge tail and differential elevon for roll, b) baseline wing w/ thin vertical and wing mounted ailerons for roll, c) large delta wing w/ thin vertical, d) large delta wing w/ triple wedge verticals

V. Conclusions

In this paper, we developed an aerodynamic database for the North American X-15 and proposed alternatives. The handling qualities screening parameters that we track: Short-Period frequency, Dutch-Roll frequency, elevator to trim, *Cnβdynamic* and *LCDP* confirm a stable and controllable aircraft under atmospheric flight condition for the baseline X-15 and for the proposed X-15-3 configuration with large triple wedge verticals. We can see that the configuration choice of differential elevon for roll and a large dorsal wedge tail on the actual X-15 was needed to ensure that the airframe was both stable and aerodynamically controllable for its design mission. Absent these features, the vehicle would remain notionally stable in pitch and yaw, but would prove spin prone over much of its flight time because of excessive adverse yaw from conventional wing mounted roll control effectors. Similarly, a delta wing X-15 variant needs even more static directional stability to overcome the inherent dihedral effect of its swept planform. While strong aerodynamic dihedral helps stabilize the Dutch Roll mode, it exasperates the problem of adverse yaw from wing mounted elevons. Absent very large dorsal vertical stabilizing fins which retain their effectiveness at high Mach numbers (i.e. wedge tails), this configuration also proves uncontrollable in terms of its fundamental aerodynamics.

Acknowledgements

This research was supported in part by an appointment to the Postgraduate Research Participation Program at the U.S. Air Force Institute of Technology, administered by the Oak Ridge Institute for Science and Education through an interagency agreement between the U.S. Department of Energy and AFIT.

©2023 –TT Takahashi & JA Griffin

References

[1] North American Aviation, "USAF Series X-15 Aircraft Interim Flight Manual," 18 March 1960.

[2] Griffin, J. A. and Takahashi, T.T., "Aero-Spaceplane Mission Performance Estimations Incorporating Atmospheric Control Limits," AIAA 2022-3656, 2022.

[3] 1976 Standard Atmosphere

[4] Anon. "Proceedings of the X-15 First Flight 30th Anniversary Celebration." NASA CP-3105, 1989.

[5] Jenkins, D.R. and Landis, T.R., *Hypersonic: The Story of the North American X-15*, Specialty Press, North Branch, MN, 2003.

[6] Anon., "X-15 Research at the Edge of Space," NASA EP-9, 1964.

[7] Griffin, Jack, A. M.S. thesis, "A "Mission Code" Approach to Conceptual Design of Hypersonic Vehicles,"Arizona State University, Tempe, AZ, April 2022.

[8] Miranda, L.R., Baker, R.D., and Elliot, W.M., "A Generalized Vortex Lattice Method for Subsonic and Supersonic Flow", NASA CR 2875, 1977.

[9] Feagin, R. C., and Morrison,W. D., "Delta Method, An Empirical Drag Buildup Technique," Lockheed-California Co., Rept. LR-27975-VOL-1, 1978.

[10] Souders, T.J. and Takahashi, T.T., "VORLAX 2020: Making a Potential Flow Solver Great Again," AIAA 2021-2458, 2021.

[11] Weill, J. "Review of the X-15 Program," NASA TN D-1278, 1962.

[12] Walker, H.J. and Wolowicz, C.H. "Stability and Control Derivative Characteristics of the X-15 Airplane," NASA TM-X-714, 1962.

[13] White, R.M., "Resume of Handling Qualities of the X-15 Airplane," NASA TM X-715, 1962.

[14] Franklin, A.E., and Lust, R.M., "Investigation of the Aerodynamic Characteristics of a 0.067-Scale Model of the X-15 Airplane (Configuration 3) at Mach Numbers of 2.29, 2.98, and 4.65," NASA TM-X-38, 1958.

[15] Osborne, Robert S., "Stability and Control Characteristics of a 0.0667-scde Model of the Final Version of the North American X-15 Research Airplane (Configuration 3) at Transonic Speeds," NASA TM X-738, 1962.

[16] Penland, Jim A. and Fetterman, David E., Jr. "Static Longitudinal, Directional, and Lateral Stability and Control Data at a Mach Number of 6.83 of the Final Configuration of the X-15 Research Airplane," NASA TM X-236, 1960.

[17] Walker, H.J. and Wolowicz, C.H. "Theoretical Stability Derivatives for the X-15 Research Airplane at Supersonic and Hypersonic Speeds Including a Comparison with Wind Tunnel Results," NASA TM X-287, 1962.

[18] Penland, J.A., Ridyard, H.W. and Fetterman, D.E., Jr. "Lift, Drag and Static Longitudinal Stability Data from an Exploratory Investigation at a Mach Number of 6.86 of an Airplane Configuration having a Wing of Trapezoidal Planform," NACA RM 54L03b, 1955.

[19] Saltzman, E.J. and Garringer, D.J. "Summary of Full-Scale Lift and Drag Characteristics of the X-15 Airplane," NASA TN D-3343, March 1966.

[20] Saltzman, E.J., "Preliminary Full-Scale Power-Off Drag of the X-15 Airplane for Mach Numbers from 0.7 to 3.1," NASA TM-X-430, 1960.

[21] Anon., "Flying Qualities of Piloted Airplanes," MIL STD-8785C, U.S. Department of Defense, Washington, D.C., November 5,1980.

[22] Takahashi, T.T., Aircraft Performance and Sizing, Volume II: Applied Aerodynamic Design, Momentum Press, New York, 2016.

[23] Day, R.E. "Coupling Dynamics in Aircraft Design: A Historical Perspective," NASA SP-532, NASA, 1997.

[24] Jarvis, C.R. and Lock, W.P. "Operational Experience With The X-15 Reaction Control And Reaction Augmentation Systems" NASA TN D-2864, 1965.

[25] Banner, R.D., Kuhl, A.E. and Quinn, R.D. "Preliminary Results of Aerodynamic Heating Studies on the X-15 Airplane," NASA TM X-638, 1962.

[26] Holleman, E.C. "Summary of High-Altitude and Entry Flight Control Experience with the X-15 Airplane", NASA TN D-3386, April 1966.

©2023 –TT Takahashi & JA Griffin